PHYSICAL REVIEW A **89**, 031802(R) (2014)

Concept of a reflective power limiter based on nonlinear localized modes

Eleana Makri, Hamidreza Ramezani, and Tsampikos Kottos
Department of Physics, Wesleyan University, Middletown, Connecticut 06459, USA

Ilya Vitebskiy
Air Force Research Laboratory, Sensors Directorate, Wright Patterson AFB, Ohio 45433, USA

(Received 23 August 2013; published 19 March 2014)

Optical limiters are designed to transmit low-intensity light, while blocking the light with excessively high intensity. A typical passive limiter absorbs excessive electromagnetic energy, which can cause its overheating and destruction. We propose the concept of a photonic reflective limiter based on resonance transmission via a localized mode. Such a limiter does not absorb the high-level radiation, but rather reflects it back to space. Importantly, the nearly total reflection occurs within a broad frequency range and direction of incidence. The same concept can be applied to infrared and microwave frequencies.

DOI: 10.1103/PhysRevA.89.031802 PACS number(s): 42.25.Bs, 42.65.−k

The continuing integration of optical devices into modern technology has led to the development of an ever increasing number of novel schemes for efficiently manipulating the amplitude, phase, polarization, or direction of optical beams [1]. Among these manipulations, the ability to control the intensity of light in a predetermined manner is of the utmost importance, with applications ranging from optical communications to optical computing [2,3] and sensoring. As laser technology progresses, novel protection devices (optical limiters) are needed to protect optical sensors and other components from high-power laser damage [4–9].

Here we focus on the most popular, passive optical limiters. The simplest realization of a passive optical limiter is provided by a single nonlinear layer with the imaginary part ϵ'' of its permittivity being dependent on the light energy density $\mathcal{W}$. At low incident energy densities, the value $\epsilon''(\mathcal{W})$ is relatively small, and the nonlinear layer is transparent. As the light intensity increases, the value $\epsilon''(\mathcal{W})$ also increases, and the nonlinear protective layer turns opaque. The physical reason for the increase in $\epsilon''(\mathcal{W})$ as a function of $\mathcal{W}$ can be different in different nonlinear optical materials. It can be two-photon absorption, photoconductivity, heating, or a combination of the above mechanisms. Specific examples of such nonlinear optical materials can be found in Refs. [7–9] and references therein. In more sophisticated schemes, the nonlinear layer can be a part of a complicated optical setup. The problem though is that in all cases, the nonlinear limiter absorbs the excessive power, which might cause overheating or even destruction of the device (a sacrificial limiter). Our goal is, using the existing nonlinear materials, to design a photonic structure that would reflect the excessive power back to space, rather than absorbing it. A free-space realization of such a reflective limiter is supposed to reflect a high-intensity radiation within a broad frequency range and regardless of the direction of incidence.

Our proposal is based on the phenomenon of resonant transmission through a localized (defect) mode. The localized mode frequency lies inside a photonic band gap of the underlying photonic structure. The simplest realization of our approach is illustrated in Fig. 1, where a nonlinear defect layer is sandwiched between two linear lossless Bragg mirrors. If the light energy density $\mathcal{W}$ is low, the imaginary part $\epsilon''(\mathcal{W})$ of the permittivity of the nonlinear defect layer can be neglected, and the defect can support a localized mode. As a consequence, at low light intensities, the layered structure in Fig. 1 will be transmissive in the vicinity of the localized mode frequency. If the incident light intensity grows, so does the value $\epsilon''(\mathcal{W})$. Eventually, the increase in $\epsilon''(\mathcal{W})$ decouples the two Bragg mirrors in Fig. 1, and the entire stack becomes highly reflective, not opaque, as in the case of a standalone nonlinear layer. In other words, the high-intensity light will be reflected back to space, rather than absorbed by the limiter. Even this simple design can provide protection from high-level radiation within a broad frequency range and for an arbitrary direction of incidence. For a given material of the nonlinear defect layer, the incident light intensity at which the structure in Fig. 1 becomes highly reflective can be controlled by the proper design of the Bragg mirrors. A problem with the simple design of Fig. 1 is that the low-intensity transmittance occurs only in the vicinity of the localized mode frequency. This problem can be addressed by using more sophisticated photonic structures, for instance, those involving two or more coupled defect layers, as is done in the case of optical filters [10].

To illustrate our idea, we consider a pair of identical Bragg mirrors, each consisting of two alternating layers with real permittivities ϵ_1 and ϵ_2, placed in the intervals $-L \leqslant z \leqslant 0$ and $d_\gamma \leqslant z \leqslant L + d_\gamma$. The width of each layer is d. A nonlinear lossy layer of width d_γ is placed between the two mirrors at $0 \leqslant z \leqslant d_\gamma$; its complex permittivity $\epsilon_\gamma = \epsilon[1 + i\gamma|E(z)|^2]$ is field dependent. In the particular case of $\epsilon = \epsilon_1$ and $\gamma = 0$, we have a standard Bragg mirror with a band gap around the frequency $\omega_B = c/(n_0 d)$ (c is the speed of light). The defect layer creates a localized mode with the frequency ω_r lying within a photonic band gap. At this frequency, the entire stack displays resonance transmission accompanied by a dramatic field enhancement in the vicinity of the defect layer. The enhanced field, in turn, causes the respective increase in the imaginary part of the defect layer permittivity, ϵ_γ. The latter will eventually result in decoupling of the two Bragg reflectors and rendering the entire structure in Fig. 1 highly reflective.

We first consider normal incidence. In this arrangement, a time-harmonic electric field of frequency ω obeys the

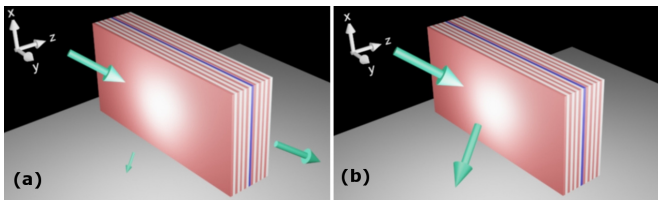

FIG. 1. (Color online) A power limiter consisting of a nonlinear lossy layer (blue layer) embedded in a Bragg mirror (white and orange layers). This setup provides (a) a resonant transmission of a low intensity light and (b) nearly total reflectivity of a high-intensity light.

Helmholtz equation:

$$\frac{\partial^2 E(z)}{\partial z^2} + \frac{\omega^2}{c^2}\epsilon(z)E(z) = 0. \tag{1}$$

Eq. (1) admits the solution $E_0^-(z) = E_f^- \exp(ikz) + E_b^- \exp(-ikz)$ for $z < -L$ and $E_0^+(z) = E_f^+ \exp(ikz) + E_b^+ \exp(-ikz)$ for $z > L + d_\gamma$ where the wave vector $k = n_0\omega/c$. The transmittance, reflectance, and absorption, e.g., for a left incident wave, are then defined as $\mathcal{T} = |E_f^+/E_f^-|^2$; $\mathcal{R} = |E_b^-/E_f^-|^2$; and $\mathcal{A} = 1 - \mathcal{T} - \mathcal{R}$, respectively [11]. They can be calculated numerically using a backward map approach [12].

The amplitudes of forward and backward propagating waves on the left $z < -L$ (right $z > L + d_\gamma$) domains outside of the Bragg mirror are related to the ones before (after) the nonlinear impurity layer by the relations:

$$\begin{pmatrix} E_f^b \\ E_b^b \end{pmatrix} = M^{(L)} \begin{pmatrix} E_f^- \\ E_b^- \end{pmatrix}; \quad \begin{pmatrix} E_f^+ \\ E_b^+ \end{pmatrix} = M^{(R)} \begin{pmatrix} E_f^a \\ E_b^a \end{pmatrix}, \tag{2}$$

where $M^{(L)}$ ($M^{(R)}$) are the 2×2 transfer matrices of the optical structure associated with the domain $-L \leqslant z \leqslant 0$ ($d_\gamma \leqslant z \leqslant L + d_\gamma$). Above we have expressed the field before (after) the nonlinear layer as $E^b = E_f^b \exp(ikz) + E_b^b \exp(-ikz)$ [$E^a = E_f^a \exp(ikz) + E_b^a \exp(-ikz)$]. The field $E^a(z = d_\gamma)$ and its derivative $(dE^a/dz)|_{z=d_\gamma}$ just after the nonlinear layer is then evaluated using $M^{(R)}$ from Eq. (2) together with the boundary conditions (associated with a left incident wave) $E_b^+ = 0$ and $E_f^+ = 1$. Using $E^a(z = d_\gamma)$ and $[dE^a(z)/dz]|_{z=d_\gamma}$ as boundary conditions we have integrated backwards Eq. (1), with the help of a fourth-order Runge-Kutta algorithm, and obtained the field $E^b(z = 0)$ and its derivative $(dE^b/dz)|_{z=0}$ at the other end $z = 0$ of the nonlinear layer. From these values we evaluate the forward E_f^b and backward E_b^b propagating amplitudes. Utilizing Eq. (2) together with $M^{(L)}$ we finally find the amplitudes E_f^- and E_b^-, which allow us to calculate $\mathcal{T}$,$\mathcal{R}$, and $\mathcal{A}$. Note that for a backward map with boundary condition $E_f^+ = 1$ we have $|E_f^-|^2 = 1/\mathcal{T}$.

It is convenient to work with the rescaled variable $\tilde{E}(z) = \sqrt{\gamma}E$. In this representation, Eq. (1) becomes

$$\frac{\partial^2 \tilde{E}(z)}{\partial z^2} + \frac{\omega^2}{c^2}\tilde{\epsilon}(z)\tilde{E}(z) = 0, \tag{3}$$

where $\tilde{\epsilon}(z \notin [0,d_\gamma]) = \epsilon(z)$, while $\tilde{\epsilon}(z \in [0,d_\gamma]) = \epsilon_\gamma(1 + i|\tilde{E}(z)|^2)$. In other words, in this representation, the nonlinear layer has a fixed absorption rate which is equal to unity, the outgoing field boundary associated with the backward map varies as $\tilde{E}_f^+ = \sqrt{\gamma}$ while the incident light energy density is $\mathcal{W}_I \equiv |\tilde{E}_f^-|^2 = \gamma/\mathcal{T} = \gamma|E_f^-|^2$.

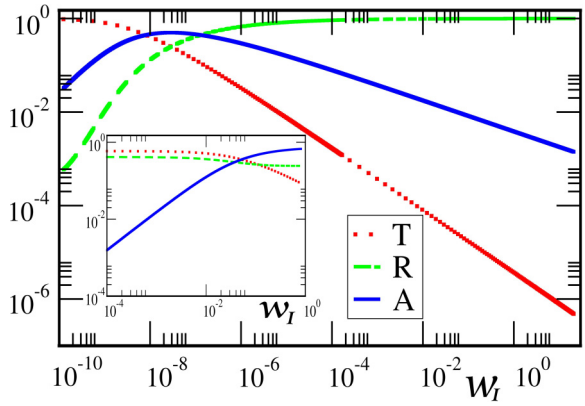

FIG. 2. (Color online) Normal incidence for the structure of Fig. 1. We report the transmittance $\mathcal{T}$, absorption $\mathcal{A}$, and reflectance $\mathcal{R}$, as a function of the energy density of the incident light $\mathcal{W}_I$ at a resonant frequency $\omega_r \approx 8.15$. The parameters of the one-dimensional photonic band-gap structure are indicated at the text. We observe that for moderate values of $\mathcal{W}_I$, both $\mathcal{T}$ and $\mathcal{A}$ are suppressed and the system becomes reflective, i.e., $\mathcal{R} \approx 1$. Inset: $\mathcal{T}$, $\mathcal{A}$, $\mathcal{R}$ for a single nonlinear layer (normal incidence). This system, for moderate $\mathcal{W}_I$ values, does not reflect but mainly absorbs the incident energy.

In Fig. 2 the effect of the incident intensity $\mathcal{W}_I$ on the transmission, reflection and absorption of a resonant localized mode is presented. The one-dimensional photonic band gap medium used in these simulations consists of 40 layers on each side with alternating permittivities $\epsilon_1 = 4$ and $\epsilon_2 = 9$. The width of the impurity layer is $d_\gamma = 1$ and the amplitude ϵ of the nonlinear permittivity is $\epsilon = 9$. We have confirmed numerically that in the linear case the defect creates a resonant mode at $\omega_r \approx 8.15$ [13] at the band gap of the Bragg mirrors, which is localized around the impurity. We find that as the incident light energy density $\mathcal{W}_I$ increases (main panel of Fig. 2), the transmittance of this resonant mode decreases, with a simultaneous increase of the absorption. Further increase of $\mathcal{W}_I$, results in noticeable growth of the reflectance with a simultaneous decrease of the absorption and transmittance. Eventually both $\mathcal{T}$ and $\mathcal{A}$ vanish for moderate values of $\mathcal{W}_I$. In other words the system reflects completely the incident radiation. For the shake of comparison we also calculated $\mathcal{T}$,$\mathcal{A}$, and $\mathcal{R}$ versus $\mathcal{W}_I$ for a single nonlinear layer with no Bragg reflectors (see inset of Fig. 2). We find that for the same range of moderate values of $\mathcal{W}_I$, the system rather absorbs the energy instead of reflecting it back to space.

For normal incidence, a further theoretical analysis based on the so-called backward mapping [12] can be carried out. To this end we assume that the permittivity of the nonlinear layer is $\epsilon_\gamma(z) = \epsilon[1 + i\gamma|E(z)|^2]\delta(z)$. This approximation is justified in the case of a *thin* metallic defect. For the analytical calculation of $\mathcal{T}$,$\mathcal{R}$, and $\mathcal{A}$, we proceed along the same lines that we have highlighted in the numerical analysis previously. For the sake of generality we will assume that the transport characteristics of the left and right linear subsystems are encoded in the values of their left (right) transmission $t_L(t_R)$ and reflection $r_L(r_R)$ amplitudes. The elements of the transfer

matrices $M^{(L)}$ and $M^{(R)}$ [see Eq. (2)] are defined as $M_{11}^{(L/R)} = 1/t_{L/R}^*$, $M_{12}^{(L/R)} = -r_{L/R}/t_{L/R}$, $M_{21}^{(L/R)} = -(r_{L/R}/t_{L/R})^*$, and $M_{22}^{(L/R)} = 1/t_{L/R}$. We remark that bistabilities are present for a very narrow parameter range of the system and therefore can be omitted from our considerations below.

Next we calculate the field amplitudes just before and after the delta defect by utilizing the transfer matrices Eq. (2) associated with the linear segments. For a left incident wave, we have at $z = 0^-$

$$E_f^b = \frac{E_f^-}{t_L^*} - \frac{r_L E_f^+}{t_L}; \quad E_b^b = \frac{E_f^+}{t_L} - \frac{E_f^- r_L^*}{t_L^*}, \tag{4}$$

while at $z = 0^+$ just after the delta defect we have

$$E_f^a = \frac{t_R^* E_f^+}{1 - |r_R|^2}; \quad E_b^a = \frac{t_R r_R^* E_f^+}{1 - |r_R|^2}. \tag{5}$$

Using Eqs. (4) and (5) together with the continuity of the field at $z = 0$ and the suitable discontinuity of its derivative we write the incident and reflected field amplitudes in terms of the transmitted wave amplitude

$$\begin{aligned} E_f^- &= \left\{ \frac{1}{\tau_0} - i\left(\frac{1}{\tau} - \frac{1}{\tau_0}\right)\gamma|\xi|^2|E_f^+|^2 \right\} E_f^+, \\ E_b^- &= \left(\frac{t_L}{1 - r_L}\right)\left\{ \xi E_f^+ - \frac{(1 - r_L^*)}{t_L^*} E_f^- \right\}, \end{aligned} \tag{6}$$

where τ is the transmission amplitude in the absence of the δ-like layer, τ_0 is the transmission amplitude when $\gamma = 0$, and $\xi = \frac{t_R^* + t_R r_R^*}{1 - |r_R|^2}$. From Eq. (6) we deduce the transmission, reflection and absorption amplitudes. For the transmission and reflection amplitude we get that

$$\begin{aligned} t &= \frac{1}{\frac{1}{\tau_0} - i\left(\frac{1}{\tau} - \frac{1}{\tau_0}\right)\gamma|\xi|^2|E_f^+|^2}, \\ r &= \left(\frac{t_L}{1 - r_L}\right)\left\{ t\xi - \frac{1}{t_L^*}(1 - r_L^*) \right\}. \end{aligned} \tag{7}$$

The transmittance, reflectance, and absorption can then be calculated as $\mathcal{T} = |t|^2, \mathcal{R} = |r|^2$, and $\mathcal{A} = 1 - \mathcal{T} - \mathcal{R}$. From Eq. (7) we observe that increasing γ (we note that the energy density of the incident light $\mathcal{W}_I \sim \gamma$) results in an increase of the denominator of the transmission amplitude and therefore to a decrease of $\mathcal{T}$ (for very large γ values it becomes zero). At the same time the reflection amplitude, becomes $r \to (\frac{t_L}{1 - r_L})\{-\frac{1}{t_L^*}(1 - r_L^*)\}$ corresponding to perfect reflection, i.e., $\mathcal{R} \to 1$. Consequently in this limit we have zero absorption $\mathcal{A} = 0$.

Figure 3 demonstrates the effect of $\mathcal{W}_I$ on a resonant localized mode for the case of symmetrically placed Bragg mirrors on the left and right side of a δ-like defect. The alternate layers at the Bragg mirrors have permittivity $\epsilon_1 = 4$ and $\epsilon_2 = 9$ while the permittivity of the defect layer is $\epsilon = 1.5$. The transport characteristics of the Bragg mirrors $t_L = t_R$ and $r_L = r_R$ have been calculated numerically and used as inputs in Eqs. (7). We find (see Fig. 3) that the overall behavior of $\mathcal{T}, \mathcal{R}$, and $\mathcal{A}$ is similar to the one observed in the simulations of Fig. 2.

For comparison, we also report (inset of Fig. 3) the behavior of $\mathcal{T}, \mathcal{A}$, and $\mathcal{R}$, for a single nonlinear layer (without any Bragg mirrors), vs the incident light energy density $\mathcal{W}_I$. They are calculated analytically using the continuity of the field and the discontinuity of its derivative at the position of the δ defect. Specifically, $\mathcal{T} = \frac{4}{(k\epsilon_0)^2 + (2 + k\epsilon_0\gamma|E_f^+|^2)^2}$; $\mathcal{R} = (k\epsilon_0)^2(1 + \gamma^2|E_f^+|^4)\mathcal{T}/4$ and $\mathcal{A} = k\epsilon_0\gamma|E_f^+|^2\mathcal{T}$. We find that for moderate $\mathcal{W}_I$ values the single nonlinear layer is mainly absorptive (inset of Fig. 3) while the structure of Fig. 1 is mainly reflecting the incident light back to space (main panel of Fig. 3).

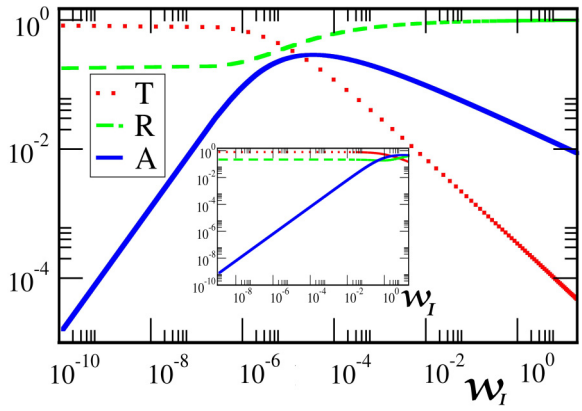

FIG. 3. (Color online) Transport characteristics for the model of a nonlinear δ-like defect embedded in a Bragg mirror. The theoretical results of Eq. (7) shown here, reproduce nicely the features of the simulations reported in Fig. 2. In the inset we report, for comparison, $\mathcal{A}, \mathcal{T}$, and $\mathcal{R}$ for a single nonlinear layer. We assume normal incidence at $\omega = 0.7 \approx \omega_r$.

We have also investigated the efficiency of the proposed limiter in the case of oblique incidence. A representative example in the case of an incident angle $\phi = 6^\circ$ is shown in Fig. 4. The Bragg mirror considered in this example consists of two layers with permittivities $\epsilon_1 = 9$, $\epsilon_2 = 16$ while the

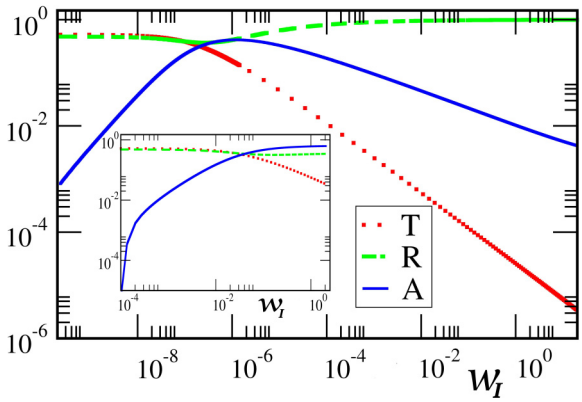

FIG. 4. (Color online) Simulations for the structure of Fig. 1 for oblique incidence at $\omega = 8.95 \approx \omega_r$. The parameters of the Bragg mirror are indicated at the text while the incident angle is $\phi = 6^\circ$. We find that for moderate values of the energy density of the incident light $\mathcal{W}_I$, the transmittance and absorption are suppressed and the system is reflective, i.e., $\mathcal{R} = 1$. In the inset we report for comparison (and for the same range of $\mathcal{W}_I$ values) the $\mathcal{A}$, $\mathcal{T}$, and $\mathcal{R}$ values for the case of a single nonlinear layer. This system mainly absorbs the incident energy.

nonlinear impurity has permittivity $\epsilon = 16$. We find again that as the incident light energy density $\mathcal{W}_I$ takes moderate values, the transmittance and the absorption are suppressed, and the structure becomes reflective, i.e., $\mathcal{R} \approx 1$. This behavior has to be contrasted with the one found for the single nonlinear layer where for moderate $\mathcal{W}_I$ values the dominant mechanism is absorption; see the inset of Fig. 4.

The effectiveness of the structure of Fig. 1 to act as a self-protecting power limiter for any incident angle calls for a generic argument for its explanation. The following heuristic argument, provides some understanding of the mechanism underlying our structure. First we recall that the defect results in the creation of a resonance mode which is localized around the impurity layer at $z = 0$ and decays away from its localization center with an envelope profile $E_r(z) \sim \exp(-\alpha|z|)$ (all distances are measured in units of the width layer d). An incoming (say from the left) wave that carries an incident energy flux $\mathcal{S}$ can resonate via this mode as long as the loss coefficient is $\gamma \leqslant \gamma^* \sim \mathcal{S}/\mathcal{W}_0 \sim \exp(-2\alpha L)$ [$\mathcal{W}_0 \sim |E_r(z=0)|^2 \sim \exp(2\alpha L)$ is the mode energy density at $z = 0$ [14]]. In other words, the energy that is absorbed from the nonlinear lossy layer via the resonant mode cannot be more than the incoming energy. Therefore for any $\gamma > \gamma^*$ the resonant mode will not be sustained, and thus the transmission $\mathcal{T}$ will be exponentially small.

We proceed in our argument by noticing that the resonant mode is located at the band gap of the Bragg mirror, and therefore it can be written as a superposition of two evanescent modes, one growing and another one decaying; i.e., $E_r(z) \sim \psi_+(z) + \psi_-(z)$, where $\psi_- \sim \alpha_- \exp(-z)$ and $\psi_+ \sim \alpha_+ \exp(z)$. Let us assume that $\alpha_+ \sim O(1)$ [15]. Then the field at the outer boundary of the left mirror at $z = -L$ is $E_r(z = -L) = \alpha_+ \exp(-L) + \alpha_- \exp(L) \sim \alpha_- \exp(L)$. At the same time due to continuity at the boundary we expect that the resonance wave function must be equal to the incoming field, which we assume to take some constant value, i.e., $\alpha_- \exp(L) \sim O(1)$. This can only happen if $\alpha_- \to 0$. Finally we recall that the incoming energy flux is given by the Poynting vector $\mathcal{S}$, which in the case of evanescent modes is $S \sim \psi_+\psi_- = \alpha_+\alpha_- \to 0$ [16]. Therefore there will be no net flux towards the structure, and thus $\mathcal{A} \approx 0$. Since $\mathcal{T} \approx 0$ and $\mathcal{A} \approx 0$, we conclude that most of the incident light energy is reflected back, i.e., $\mathcal{R} \approx 1$.

We have examined the scattering problem for a periodic layered structure with an embedded nonlinear defect. We presume that the imaginary part ϵ'' of the permittivity of the defect layer increases with the light energy density, which is normally the case. We have shown that such a layered structure can act as a reflective power limiter. Specifically, at low intensity of the incident light, the entire stack is highly transmissive in the vicinity of the localized mode frequency. When the input power exceeds a certain level, the nonlinearity suppresses the localized mode, and the layered structure becomes highly reflective (not absorptive!) within a broad frequency range and for a wide direction of incidence. In other words, the excessively strong radiation will be reflected back to space, rather than being absorbed by the lossy nonlinear layer. This can prevent overheating and destruction of the limiter. A simple realization of such a self-protected (reflective) power limiter is provided by a lossy nonlinear layer sandwiched between two Bragg mirrors, as shown in Fig. 1. A shortcoming of such a simple design is that although the high-intensity radiation will be reflected back to space within a broad frequency range, the low-intensity transmittance occurs only within a narrow frequency band in the vicinity of the localized mode frequency. This problem can be addressed by using a more sophisticated layered structure than that shown in Fig. 1.

The above approach to the realization of a reflective power limiter is perfectly scalable and can be applied to any frequency range. Of course, the structural geometry and the material choice of the nonlinear layer and the Bragg reflectors are all dependent on the frequency of interest and on the light intensity limitations. For instance, the material of choice for the nonlinear defect layer can be ZnSe (at optical frequencies) and InP or GaAs (at near-infrared frequencies) [7–9]. The Bragg reflectors can be made of alternate layers of silicon nitride (Si_3N_4) and silica (SiO_2). For a given nonlinear defect layer, the incident light intensity at which the whole structure in Fig. 1 turns from transmissive to highly reflective is strongly dependent on the number of layers in the Bragg reflectors. An experimental realization of this setup is currently under investigation.

This work is partly sponsored by the Air Force Research Laboratory (AFRL/RYDP) through the AMMTIAC contract with Alion Science and Technology, and by the Air Force Office of Scientific Research LRIR09RY04COR and FA 9550-10-1-0433 and by an AFOSR MURI grant FA9550-14-1-0037.

[1] B. E. A. Saleh and M. C. Teich, *Fundamentals of Photonics* (Wiley, New York, 1991).

[2] T. Ohtsuki, J. Lightwave Technol. **15**, 452 (1997).

[3] N. S. Patel, K. L. Hall, and K. A. Rauschenbach, Appl. Opt. **37**, 2831 (1998).

[4] L. W. Tutt and T. F. Boggess, Prog. Quant. Electr. **17**, 299 (1993); A. E. Siegman, Appl. Opt. **1**, 739 (1962); J. E. Geusic, S. Singh, D. W. Tipping, and T. C. Rich, Phys. Rev. Lett. **19**, 1126 (1967).

[5] Y. Zeng, X. Chen, and W. Lu, J. Appl. Phys. **99**, 123107 (2006); M. Scalora, J. P. Dowling, C. M. Bowden, and M. J. Bloemer, Phys. Rev. Lett. **73**, 1368 (1994).

[6] S. Husaini *et al.*, Appl. Phys. Lett. **102**, 191112 (2013); S. Pawar *et al.*, J. Nonlin. Opt. Phys. Mat. **21**, 1250017 (2012).

[7] J. M. Ralston and R. K. Chang, Appl. Phys. Lett. **15**, 164 (1969); V. V. Arsenev, V. S. Dneprovksii, D. N. Klyshko, and A. N. Penin, Sov. Phys. JETP **29**, 413 (1969).

[8] T. F. Boggess, A. L. Smirl, S. C. Moss, I. W. Boyd, and E. W. Van Stryland, IEEE J. Quantum Electron. **21**, 488 (1985); T. F. Boggess, S. C. Moss, I. W. Boyd, and A. L. Smirl, Opt. Lett. **9**, 291 (1984).

[9] M. D. Dvorak and B. L. Justus, Opt. Comm. **114**, 147 (1995).
[10] H. A. Macleod, *Thin-Film Optical Filters* (Institute of Physics Publishing, Bristol, 2001).
[11] The quantities $\mathcal{T},\mathcal{R},\mathcal{A}$ are the same for a right incident wave as well, since our structure is reciprocal.
[12] E. Lidorikis, K. Busch, Q. Li, C. T. Chan, and C. M. Soukoulis, Phys. Rev. B **56**, 15090 (1997); G. Tsironis and D. Hennig, Phys. Rep. **307**, 333 (1999).
[13] In all numerical simulations in Figs. 2–4 we use units such that $c = 1$, $d = 1$.
[14] We assume the incident wave has amplitude $O(1)$ and that due to continuity of the wave function at the boundary $E_{\text{res}}(z = -L) \sim O(1) \rightarrow E_{\text{res}}(z = 0) \sim \exp(L)$.
[15] A similar argument can be used for $\alpha_{-} \sim O(1)$.
[16] A. Figotin and I. Vitebskiy, Waves Random Complex Media **16**, 293 (2006).